Adaptive Zero-Padding OFDM for Wireless Communications

Neng Wang and Steven D. Blostein
Department of Electrical and Computer Engineering
Queen's University, Kingston, Ontario, Canada K7L 3N6
E-mail: {nwang,sdb}@ee.queensu.ca

Abstract— **In this paper we present a novel bandwidth (BW) efficient orthogonal frequency division multiplexing (OFDM) scheme with adaptive zero-padding (AZP-OFDM) for wireless transmission. Redundancy issues in the existing cyclic prefix (CP) and zero-padding (ZP) based OFDM as well as no-guard-interval (NGI) systems are analyzed. A novel system design criterion based on the channel matrix condition is studied and applied in the design of an adaptive zero-padding (AZP) OFDM system. Simulation results show that the proposed AZP-OFDM offers performance similar to that of the CP based scheme, complexity similar to that of ZP based schemes, with BW efficiency higher than that of both CP- and ZP-OFDM. Essentially, AZP-OFDM offers a better tradeoff between symbol recovery, BW efficiency, and complexity and more flexibility for implementation.**

I. Introduction

Orthogonal Frequency Division Multiplexing (OFDM) has been receiving growing interest in recent years and has been adopted in many standards. All OFDM systems already standardized in the past are based on the conventional OFDM scheme that uses a cyclic prefix (CP). Inserting a CP of length no less than the channel order and discarding it at the receiver not only suppresses IBI, but also facilitates the diagonalization of the channel matrix, and makes single-tap equalization possible [12]. An obvious problem in CP-OFDM systems is that the transmitted symbols cannot be recovered when some channel zeros are located on subcarriers. Recently, it has been proposed in [4], [10] to replace CP insertion by zero-padding (ZP) at the end of the block of symbols to be transmitted. The padded zeros deterministically suppress the IBI and guarantee symbol recovery [12]. Note that since the number of zeros required to cancel IBI equals the CP length, ZP- and CP-OFDM transmission have the same bandwidth (BW) efficiency. For some existing OFDM systems, such as HIPERLAN/2 and DAB physical layer, the length of the CP is chosen to be 1/4 of the block size, which results in a BW efficiency of 80%.

Some approaches have been proposed to increase the BW efficiency in OFDM systems [11], [7]. In [11], an OFDM system that does not use a guard interval (we refer to as NGI-OFDM) was proposed. Equalization in such a system requires computing the Moore-Penrose pseudoinverse of the channel matrix and suffers from error floors in performance according to our analysis and simulation. In wireline applications, channel impulse response shortening techniques have been developed so that the length of guard interval can be reduced [7]. But their applications to wireless systems may be very difficult due time varying characteristic of wireless channels.

In this paper, we propose a novel OFDM transmission scheme with adaptive zero-padding (AZP-OFDM) to increase the BW efficiency. We first examine the redundancy introduced in the existing OFDM schemes. Then we investigate the possibility to reduce such redundancy and introduce a novel system design criterion based on channel matrix condition, which is shown to be able to predict system performance very well. With this criterion, a BW efficient zero-padding scheme, AZP-OFDM, is developed to tradeoff efficiency and performance. Furthermore, complexity issues are also included in system design, which results in a more flexible design in that one can make tradeoffs among performance, efficiency and complexity.

This paper is organized as follows. A brief description of the existing OFDM schemes as well as redundancy issues are provided in Section II. In Section III, we propose a system design criterion based on channel matrix condition, and its application to the design of BW efficient zero-padding OFDM systems. Simulation results and some further discussions in the context of HIPERLAN/2 channel models are provided in Section IV.

II. System Description

A. CP-OFDM

A serial stream of data, $u(n)$, is serial-to-parallel (S/P) converted into data blocks of size N, $\mathbf{u}(i) \stackrel{\text{def}}{=} [u(iN), u(iN+1), \cdots, u(iN+N-1)]^T$. Performing multicarrier modulation via inverse fast Fourier transform (IFFT), we obtain

$$\mathbf{s}(i) = \mathbf{F}^H \mathbf{u}(i)$$

where $\mathbf{F}$ is the $N \times N$ FFT matrix with $[\mathbf{F}]_{n,k} = \frac{1}{\sqrt{N}} e^{-j2\pi nk/N}$. A guard interval in terms of CP of length G is then inserted between each block, and the resulting redundant i-th block $\mathbf{s}_{cp}(i)$ of length $P = N+G$ is parallel-to-serial (P/S) converted into time-domain samples $s_{cp}(n)$ and sent sequentially through the channel. Assume perfect symbol and block synchronization. If the length of the CP, G, is no less than the channel model order, L, after

This research has been supported by the Natural Sciences and Engineering Research Council of Canada.

discarding the first G entries, which correspond to CP, we obtain

$$\mathbf{r}_{cp}(i) = \tilde{\mathbf{H}}\mathbf{s}(i) + \tilde{\boldsymbol{\eta}}_{cp}(i) \tag{1}$$

where $\tilde{\mathbf{H}}$ is the $N \times N$ circulant matrix with the first column $[h_0, \cdots, h_L, 0, \cdots, 0]^T$; and $\tilde{\boldsymbol{\eta}}_{cp}(i)$ is the $N \times 1$ AWGN vector. After demodulation by FFT, we get

$$\begin{aligned} \mathbf{y}_{cp}(i) &= \mathbf{F}\tilde{\mathbf{H}}\mathbf{F}^H\mathbf{u}(i) + \mathbf{F}\tilde{\boldsymbol{\eta}}_{cp}(i) \\ &= \mathbf{D}(H)\mathbf{u}(i) + \boldsymbol{\eta}_{cp}(i) \end{aligned} \tag{2}$$

where $\mathbf{D}(H) = \mathrm{diag}[H(0), \cdots, H(N-1)]$ with $H(n) = \sum_{l=0}^{L} h_l e^{-j2\pi nl/N}$ denoting the channel frequency response on the k-th subcarrier, and $\boldsymbol{\eta}_{cp}(i)$ is the FFT-processed noise vector.

CP-OFDM uses redundancy in the cyclic prefix to cancel IBI and transform the linear convolutional channel into a circular one, which makes simple one-tap equalization possible. One main problem in CP-OFDM systems is that the transmitted symbols cannot be recovered when some subcarriers encounter channel zeros [12].

B. ZP-OFDM

ZP-OFDM ([4], [10]) transmission differs from CP-OFDM only in that instead of CP insertion, a guard interval in terms of G zeros is padded at the end of each block. Assuming $G \geq L$, the received block symbol is given by

$$\mathbf{r}_{zp}(i) = \bar{\mathbf{H}}\mathbf{s}(i) + \boldsymbol{\eta}_{zp}(i) \tag{3}$$

where $\bar{\mathbf{H}}$ is a $P \times N$ tall Toeplitz matrix with the first column $[h_0, \cdots, h_L, 0, \cdots, 0]^T$; and $\boldsymbol{\eta}_{zp}(i)$ is the $P \times 1$ AWGN vector.

Redundancy in ZP-OFDM is introduced in terms of trailing zeros, which not only cancels IBI but also guarantees symbol recovery because the tall Toeplitz channel matrix in (3) is always well-coditioned [12]. The price to pay for this benefit is increased equalization complexity [8].

C. NGI-OFDM

An OFDM transmission scheme without using guard intervals, NGI-OFDM, was proposed in [11] to achieve maximal BW efficiency. The IBI due to time dispersion of the channel is combated by ISI cancellation as in [6]. After IBI cancellation, the "IBI-free" received block symbol is given by

$$\mathbf{r}_{ngi}(i) = \mathbf{H}\mathbf{s}(i) + \boldsymbol{\eta}_{ngi}(i) \tag{4}$$

where $\mathbf{H}$ is an $N \times N$ lower triangular Toeplitz matrix with the first column $[h_0, \cdots, h_L, 0, \cdots, 0]^T$, which cannot be diagonalized with FFT operations; and $\boldsymbol{\eta}_{ngi}(i)$ is the $N \times 1$ AWGN vector. Therefore, inter-carrier interference (ICI) has been introduced and must be mitigated for symbol detection.

Equalization in NGI-OFDM is to solve the linear equation in (4), which is probably ill-conditioned. Fig. 2 shows an example of the condition number of NGI-OFDM channel matrix varying with time in HIPERLAN/2 channel A with a terminal speed $v = 3(m/s)$. As a comparison, those of CP- and ZP-OFDM are also shown. From Fig. 2 we can see that the condition number of NGI-OFDM is usually very large, which makes equalization in (4) an ill-conditioned problem, and moreover causes unacceptable performance in NGI-OFDM, as shown in Section IV.

III. Proposed BW-Efficient ZP-OFDM Scheme

To increase the BW efficiency of ZP-OFDM systems, redundancy introduced in transmission must be reduced. Usually the tail taps of channel impulse responses are weak compared with the head part, so their effect is also weak and may be neglected without affecting overall system performance dramatically. Therefore, if we loosen the constraint on guaranteed symbol recovery slightly, higher efficiency may be achieved.

A. BW-Efficient Zero-Padding Scheme

Consider the signal model in ZP-OFDM. Rewrite (3) as

$$\mathbf{r} = \mathbf{H}\mathbf{s} + \boldsymbol{\eta} \tag{5}$$

where for convenience of notation, we have dropped subscripts and indices. Consider zero-forcing (ZF) equalization, which requires solving an overdetermined system and can be easily treated as full rank least squares (LS) problem [2]. The sensitivity of the LS problem is well measured by the condition of channel matrix $\mathbf{H}$ with respect to the 2-norm, $\kappa(\mathbf{H}) \stackrel{\text{def}}{=} \frac{\sigma_1}{\sigma_N}$, where σ_1 and σ_N denote, respectively, the maximum and minimum singular values of $\mathbf{H}$. Define the SNR at the input of the equalizer $\gamma_{in} \stackrel{\text{def}}{=} \frac{\|\mathbf{r}\|^2}{\|\boldsymbol{\eta}\|^2}$. The relative estimation error of equalization in ZP-OFDM is bounded by

$$\frac{\|\mathbf{H}^\dagger\mathbf{r} - \mathbf{s}\|}{\|\mathbf{s}\|} \leq \frac{2\kappa(\mathbf{H})}{\sqrt{\gamma_{in}}} + \mathcal{O}\left(\frac{1}{\gamma_{in}}\right). \tag{6}$$

We note that γ_{in} may range from 0 to 20 dB in wireless communications and usually $\kappa(\mathbf{H}) \gg 1$. Therefore $\mathcal{O}\left(\frac{1}{\gamma_{in}}\right)$ is usually negligible in (6). By defining the SNR at the output of the equalizer $\gamma_{out} \stackrel{\text{def}}{=} \frac{\|\mathbf{s}\|^2}{\|\mathbf{H}^\dagger\mathbf{s} - \mathbf{s}\|^2}$, we obtain approximately

$$\gamma_{out} \underset{\sim}{\geq} \frac{\gamma_{in}}{4\kappa^2(\mathbf{H})} \tag{7}$$

An example of the output SNR, γ_{out}, for ZF equalization in HIPERLAN/2 channel A is shown in Fig. 3 together with the bound in (7). The bound is not tight but gives a good prediction of γ_{out}, which in turn determine the system performance. For example, for QPSK modulation, the symbol error rate (SER) is given by [9]

$$P_s = 2Q\left(\sqrt{\gamma_{out}}\right)\left[1 - \frac{1}{2}Q\left(\sqrt{\gamma_{out}}\right)\right] \tag{8}$$

where $Q(x) \stackrel{\text{def}}{=} \frac{1}{\sqrt{2\pi}}\int_x^\infty e^{-t^2/2}dt$. Therefore, we may use $\kappa(\mathbf{H})$ as a system design criterion. To be specific, assume

K zeros are padded, with $0 \leq K \leq L$, the new signal model is given by

$$\mathbf{r}' = \mathbf{H}'\mathbf{s} + \boldsymbol{\eta}' \tag{9}$$

where $\mathbf{r}'$ and $\boldsymbol{\eta}'$ are $(N+K)$-vectors and $\mathbf{H}'$ is a $(N+K) \times N$ matrix. The corresponding channel matrix $\mathbf{H}'$ is a submatrix of the ZP-OFDM channel matrix $\mathbf{H}$ constructed by deleting its last $P-N-K$ rows. From the interlacing property of singular values and perturbation theory [5], we know that $\kappa(\mathbf{H}') \geq \kappa(\mathbf{H})$. This is the price to pay for increased BW efficiency.

Similar to ZP-OFDM, equalization in AZP-OFDM requires the solution of an overdetermined system of equations. The fast equalization algorithms developed in [8] cannot be applied due to the different structure of channel matrices.

B. Modification for Low Complexity Equalization

By taking advantage of the band-Toeplitz structure of the channel matrix, we propose a modification to the AZP-OFDM scheme. To be specific, if we discard K initial observations, we obtain a system with the same number of observations as unknowns, i.e.,

$$\mathbf{r}'' = \mathbf{H}''\mathbf{s} + \boldsymbol{\eta}'' \tag{10}$$

where $\mathbf{r}''$ and $\boldsymbol{\eta}''$ are N-vectors and $\mathbf{H}''$ is an $N \times N$ Toeplitz matrix. We note that the received signal in (10) is a "windowed" version of that in ZP-OFDM. As a result, ZF equalization is transformed into solving a band-Toeplitz system (with band width $L+1$), for which there are some efficient solvers [1].

Of course, by discarding some observations, we lose part of the redundancy in the received signal. As a result, the system performance will be slightly worse. However, due to the choice of AZP length (as will be clear in Section III-C), the resulting system is still well-conditioned, which has been confirmed by our simulations.

C. Choice of ZP Length

Since $\kappa(\mathbf{H}) = \sigma_1/\sigma_N$ and σ_N is more sensitive to perturbations, $\kappa(\mathbf{H})$ depends mainly on σ_N. Hence, instead of using condition number, we consider the smallest singular value of the channel matrix, σ_N, as a criterion. In (6), if we substitute $\kappa(\mathbf{H})$ by $\frac{1}{\sigma_N}$, we obtain approximately

$$\gamma_{out} \underset{\sim}{>} \frac{1}{4}\gamma_{in}\sigma_N^2 \tag{11}$$

An example of the approximate bound for γ_{out} is also shown in Fig. 3. From Fig. 3, we see that (11) can also predict of γ_{out} very well. Some efficient algorithms have been developed for calculating singular values of a matrix [2]. Here we adopt the power method, which can find the largest eigenvalue of a matrix $\mathbf{A}$ in absolute value and the corresponding eigenvector. To find the other ones, the power method can be applied to $(\mathbf{A}-\sigma\mathbf{I})^{-1}$ for some *shift* σ, and it will converge to the eigenvalue closest to σ. Table I details the algorithm. Now that we want to estimate the smallest singular value of $\mathbf{H}$, the power method can be applied to $(\mathbf{H}^H\mathbf{H}-\sigma^2\mathbf{I})^{-1}$ with a shit σ equals to 0 or previous estimate. Specifically, for the modified AZP-OFDM, to take the advantage of the channel matrix structure, we set $\sigma = 0$ so that in every iteration, the computational cost is mainly solving two band-Toeplitz systems, i.e., $(\mathbf{H}^H\mathbf{H})^{-1} = \mathbf{H}^{-1}\mathbf{H}^{-H}$. The convergence criterion for the power method used in our proposed method can be quite loose because we are not required to estimate the smalles singular value accurately.

Since wireless channels are well-modeled as stochastic processes, the system parameter K is random. However, it is difficult to find a closed-form expression for statistics of K. In Section IV, we will instead use simulations.

IV. Simulation Results and Discussions

Standard HIPERLAN/2 channel models [3] are used in our simulations.

A. Statistics of AZP Length

Fig. 4 shows the channel power profiles of HIPERLAN/2 channel models and the simulated probability density functions (PDFs) of AZP length, K. Since K is random, the BW Efficiency, $\mathcal{E}(K) \stackrel{\text{def}}{=} \frac{N}{N+K}$, is also random. The expected BW efficiency, $E_K[\mathcal{E}(K)] = \sum_{k=0}^{L} \frac{N}{N+k} Pr[K=k]$ using AZP-OFDM in different channels are, respectively, (A) 98.68%, (B) 97.05%, (C) 95.61%, (D) 97.87% and (E) 93.51%; while employing the standard CP- or ZP-OFDM BW efficiency is fixed at 80%. The variation of K depends on the velocity of the mobile terminal. An example of the variation of the channel matrix condition number with different numbers of padding zeros as well as variation of the estimated K with time is shown in Fig. 5 for channel A with a terminal speed of $3m/s$; the simulated transition probability matrix of K is

$$\mathbf{T} = \begin{pmatrix} 0.999 & 5\times10^{-4} & 2\times10^{-5} & 0 & 0 \\ 3\times10^{-4} & 0.999 & 3\times10^{-4} & 6\times10^{-6} & 0 \\ 6\times10^{-5} & 1.0\times10^{-3} & 0.999 & 2\times10^{-4} & 4\times10^{-6} \\ 0 & 3\times10^{-4} & 0.003 & 0.997 & 0 \\ 0 & 0 & 0 & 0.028 & 0.972 \end{pmatrix}$$

where $[\mathbf{T}]_{i,j} \stackrel{\text{def}}{=} \Pr[K(n) = i | K(n-1) = j]$ for $i, j = 0, 1, \cdots, L$. We can see that for a terminal speed of $3m/s$, the AZP length varies very slowly and it most likely changes among some neighboring values. This is due to small changes in the channel only resulting in small variations of the spectra of the channel matrix [5].

B. Complexity Issues

The above results lead to further reduction in implementation complexity of AZP-OFDM in that the AZP length need not be updated very frequently and the search algorithm is only required to examine several neighboring values, instead of performing exhaustive search over the set of all possible values. Equalization in (9) is a band Toeplitz LS problem, for which many special methods have been devised, e.g., there are several methods of complexity

$O((N+K)N)$ and even some "superfast" methods that require $O((N+K)\log N)$ operations [1]. The complexity of CP-OFDM is $O(N\log N)$, while using ZP-OFDM with fast equalization algorithms is $O(P\log P)$ [8]. In our simulations under the context of HIPERLAN/2 channel models, we estimate the AZP length every 20 blocks and the power method usually converges in several iterations. The proposed scheme has almost the same complexity as using ZP-OFDM, both of which slightly higher than that of CP-OFDM.

C. Clipping Effects

As is well-known, one of the major drawbacks of OFDM is the high peak-to-average power ratio (PAPR) of the signal to be transmitted. As a result, OFDM signals cause serious problems such as distortion of the transmitted signal due to the power amplifier (PA) non-linearity. In this paper, we consider the simplified PA model shown in Fig.1, with both input and output normalized, as in [8]. According to [8], by defining the *clipping ratio*, $\mathcal{C}$, as the number of clipped symbols over the total number of symbols, and the *Input Back-Off* (IBO) as the ratio of the mean power at PA input to the input saturation power, (which is a function of $\mathcal{C}$), the transmitter output SNR difference between CP- and ZP-OFDM is given by [8]

$$\Delta_{zp}(\mathcal{C}) = 10\log\left(\frac{P}{N}\right) + IBO_{zp}(\mathcal{C}) - IBO_{cp}(\mathcal{C})$$

Therefore, such SNR loss will be smaller with shorter guard interval, as is the case in our proposed AZP-OFDM. Since the length of AZP, K, is not fixed, we can estimate the expected SNR loss compared with CP-OFDM as

$$\overline{\Delta_{azp}}(\mathcal{C}) = E_K\left[10\log\frac{N+K}{N} + IBO_{azp}(\mathcal{C}) - IBO_{cp}(\mathcal{C})\right] \tag{12}$$

For HIPERLAN/2 transmission, Fig. 6 shows the simulated SNR loss for ZP- and AZP-OFDM with respect to CP-OFDM. The clipping effect alone requires reducing the transmit-power by less than 0.3 dB compared to CP-OFDM in order to guarantee the same amount of out-of-band radiation, while the reduction for ZP-OFDM is about 0.9 dB [8].

D. Uncoded BER performance

Fig. 7 show the uncoded BER performances of NGI-, CP-, ZP- and modified AZP-OFDM schemes in HIPERLAN/2 channel A. The AZP length is updated every 20 blocks. NGI-OFDM experiences serious error floors while AZP-OFDM has similar performance to CP-OFDM, and both slightly worse than that of ZP-OFDM. This is due to the guaranteed symbol recovery capability in ZP-OFDM, whereas for AZP-OFDM, this property has been sacrificed to achieve higher BW efficiency and lower complexity.

V. Conclusions

This paper has shown that the amount of redundancy introduced in OFDM can be used as a design parameter. A novel bandwidth efficient zero-padding scheme, AZP-OFDM, was introduced based on the channel condition, which is flexible for system design compared with the standard CP-/ZP-OFDM. A modification to AZP-OFDM offers more flexibility by considering simultaneously the bandwidth efficiency, system performance and implementation complexity. Simulations for application in wireless LANs confirm that the proposed scheme offers better tradeoff among different system specifications.

References

[1] Å. Björck, *Numerical Methods for Least Squares Problems,* SIAM, Philadelphia, 1996.

[2] J.W. Demmel, *Applied Numerical Linear Algebra,* SIAM, 1997.

[3] ETSI Normalization Committee, "Channel Models for HIPERLAN/2 in Different Indoor Scenarios," Norme ETSI, document 3ERI085B, European Telecommunications Standards Institute, Sophia-Antipolis, Valbonne, France, 1998.

[4] G.B. Giannakis, "Filterbanks for Blind Channel Identification and Equalization," *IEEE Signal Processing Letters,* vol. 4, no. 6, pp. 184–187, June 1997.

[5] R.A. Horn and C.R. Johnson, *Matrix Analysis,* Cambridge University Press, 1999.

[6] D. Kim and G.L. Stuber, "Residual ISI Cancellation for OFDM with Application to HDTV Broadcasting," *IEEE J. Select. Areas. in Comm.,* vol. 16, no. 8, pp. 1590–1599, Oct. 1998.

[7] P.J.W. Melsa, R.C. Younce and C.E. Rohrs, "Impulse Response Shortening for Discrete Multitone Transceivers," *IEEE Trans. on Communications,* vol. 44, no. 12, Dec. 1996.

[8] B. Muquet, Z. Wang, G.B. Giannakis, M. de Courville, and P. Duhamel, "Cyclic-Prefix or Zero-Padding for Multicarrier Transmissions ?," *IEEE Trans. on Communications,* (to appear) 2002.

[9] J.G. Proakis, *Digital Communications,* 3rd Ed., McGraw-Hill, 1995.

[10] A. Scaglione and G.B. Giannakis, and S. Barbarossa, "Redundant Filterbank Precoders and Equalizers - Part I & II," *IEEE Trans. on Signal Processing,* vol. 47 pp. 1988–2022, July 1999.

[11] M. Toeltsch and A.F. Molisch, "Efficient OFDM Transmission without Cyclic Prefix over Frequency-Selective Channels," *PIMRC'2000,* London, UK, 2000.

[12] Z. Wang and G.B. Giannakis, "Wireless Multicarrier Communications: where Fourier Meets Shannon," *IEEE Signal Processing Magazine,* vol. 17, no. 3, pp. 29–48, May 2000.

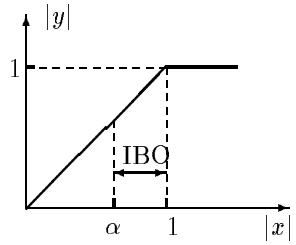

Fig. 1. Simplified Power Amplifier model.

Initialization	choose $\mathbf{x}_0$; $i=0$.
Iteration	until convergence
	$\mathbf{y}_{i+1} = (\mathbf{A}-\sigma\mathbf{I})^{-1}\mathbf{x}_i$
	$\mathbf{x}_{i+1} = \mathbf{y}_{i+1}/\\|\mathbf{y}_{i+1}\\|_2$ (approx. eigenvecotr)
	$\lambda_{i+1} = \mathbf{x}_{i+1}^H\mathbf{A}\mathbf{x}_{i+1}$ (approx. eigenvalue)
	$i = i+1$

TABLE I

Inverse Iteration of Power Method

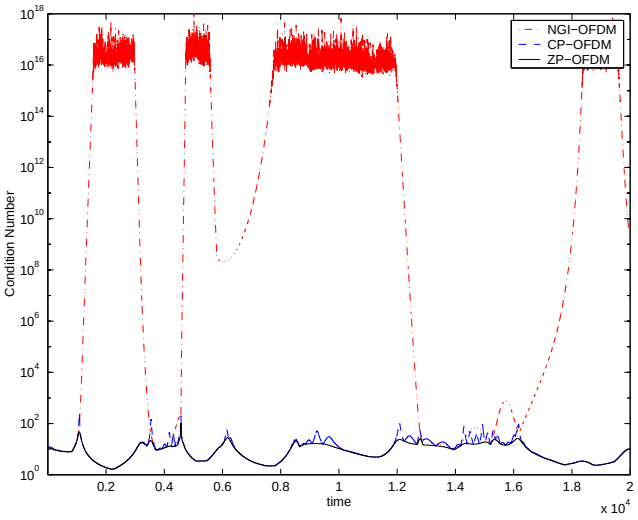

Fig. 2. Condition numbers of OFDM channel matrix vary with time in HIPERLAN/2 channel A (terminal speed $v = 3(m/s)$).

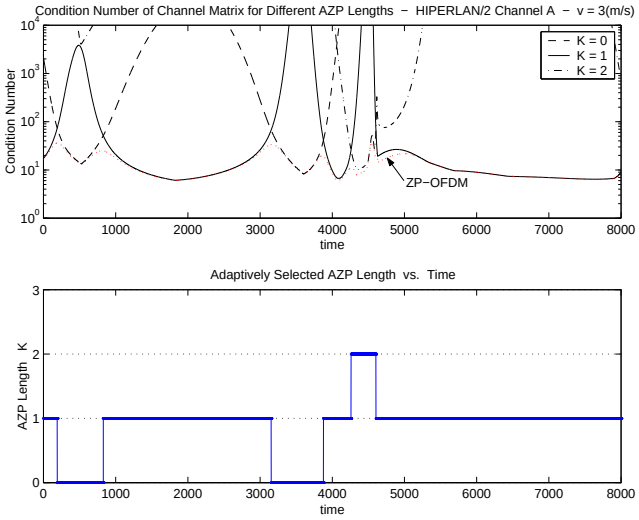

Fig. 5. Variation of AZP length with time for HIPERLAN/2 channel model A with terminal speed $v = 3(m/s)$.

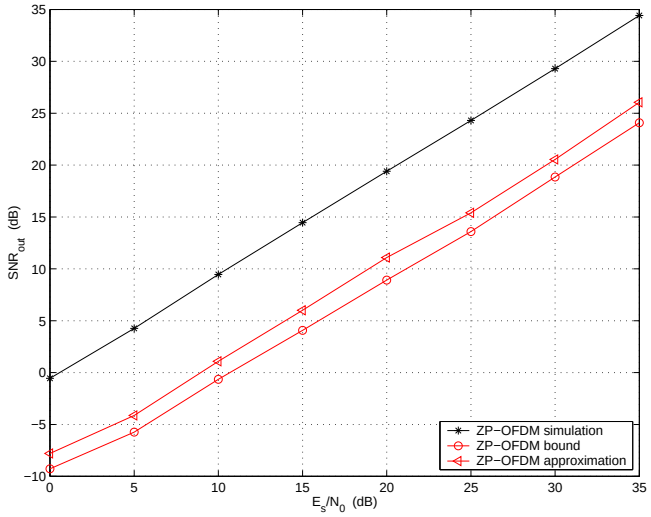

Fig. 3. Equalizer output SNR and bounds for ZF equalization in HIPERLAN/2 channel A.

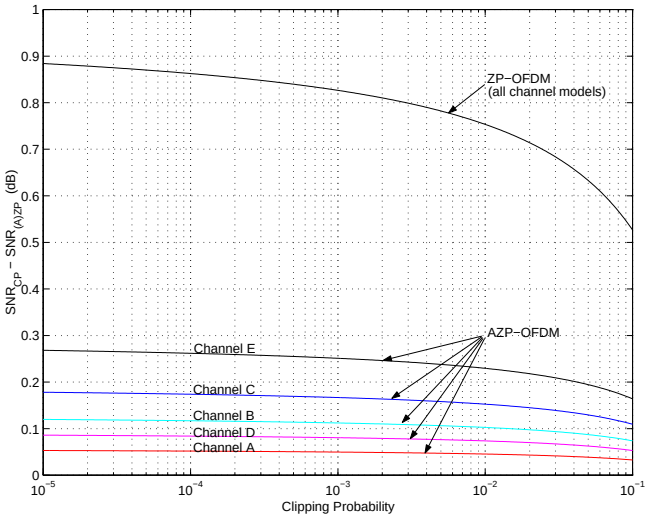

Fig. 6. SNR difference between CP and (A)ZP induced by clipping effects.

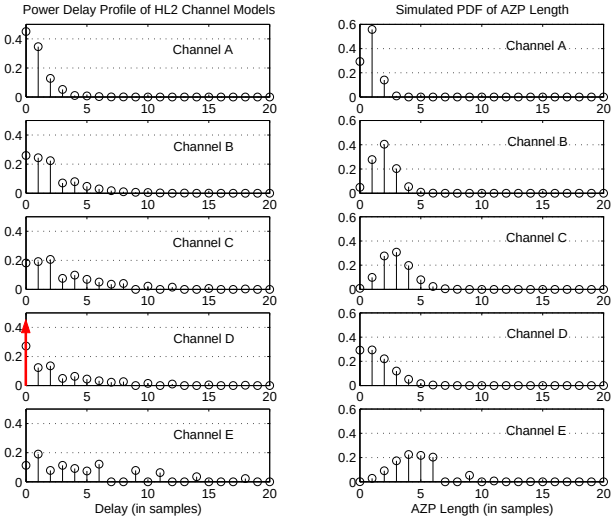

Fig. 4. HIPERLAN/2 channel power profile and simulated PDF of AZP length.

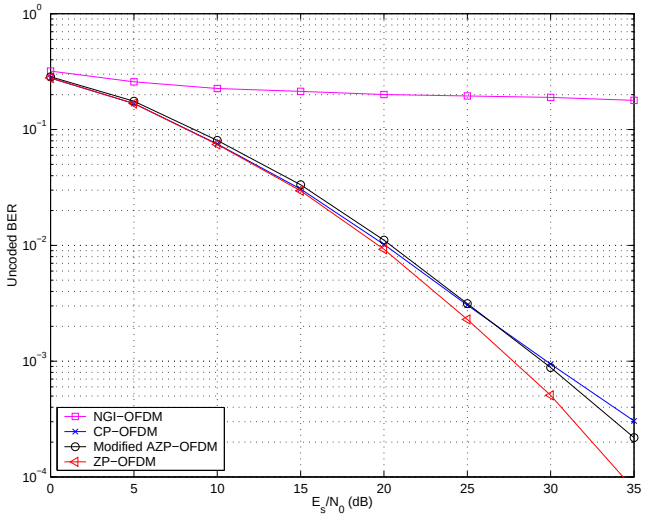

Fig. 7. Uncoded BER in HIPERLAN/2 channel A for QPSK.